USE OF COLLOCATED SENSORS TO MEASURE COASTAL WAVE REFLECTION

By David A. Huntley,[1] David Simmonds,[2] and Rao Tatavarti[3]

ABSTRACT: Two different methods for estimating frequency-dependent reflection coefficients for waves incident on a coastline using collocated measurements of elevation (or pressure) and horizontal current are investigated by simulating time series with known true reflection coefficients and added uncorrelated noise. The methods are applicable to measurements made in the nearshore zone where waves propagate essentially shore-normally. A time domain method is shown to introduce a significant positive bias in the estimated reflection coefficient. A contour plot is calculated giving the bias as a function of the estimated reflection coefficient and the coherence between the estimated incoming and outgoing wave time series, which can be used to provide corrections for the bias. A new principal component analysis (PCA) technique is found to be essentially bias-free. For this method, 95% confidence levels on zero reflection coefficient are computed for a range of numbers of degrees of freedom. Spatial separation between the sensors equivalent to a time delay, at the wave phase velocity, of τ_x produces a spurious peak with a reflection coefficient of one at frequency $1/(4\tau_x)$. The peak is very sensitive to small errors in estimating the time delay, which result in apparent reflection coefficients even higher than one. The conclusion is that the time delay must be made as small as possible in order to push the spurious peak to a high frequency. Application of these results is demonstrated using field data taken on a natural beach.

INTRODUCTION

Wave reflection from natural coastlines and man-made structures influences the hydrodynamics and the sediment dynamics in front of the reflector, and also the response of the reflector itself. It is therefore important to understand the nature of this reflection and to predict its magnitude accurately.

Much of the interest in reflection from coasts considers an average reflection coefficient appropriate to the primary incident waves. More recently, however, there has been increasing interest in the frequency-dependent reflection coefficient for a spectrum of incident waves, driven largely by the realization that the reflectivity of coasts is strongly frequency dependent, with higher frequency incident waves largely dissipated close to a structure and therefore of low reflectivity, while lower frequency waves are likely to reflect, creating a standing wave structure [Kajima (1969); Tatavarti et al. (1988); Elgar et al. (1994); and many others].

Measurements of reflectivity, both in the laboratory and in the field, have generally involved use of arrays of elevation sensors (or pressure sensors from which elevations can be calculated), where the phase differences between spatially separated sensors provides information on the shoreward or seaward propagation of the waves. Recent examples are Davidson et al. (1996) and Frigaard and Brorsen (1995). However, an alternative approach is to use collocated current and elevation/pressure sensors, where the current provides information on the slope of the sea surface from which wave propagation direction can be estimated (Guza and Bowen 1976; Tatavarti et al. 1988).

Several problems are associated with the use of arrays of elevation sensors to measure coastal reflection. One well-known problem is that singular values of reflection coefficient are calculated when the sensor spacing is equal to an integer number of half wavelengths. Another, perhaps more important, problem is that the method has to assume a predictable variation of the wave field over the scale of the array; even over simple seabed topography this may not be valid [see Baquerizo et al. (1997)].

The use of collocated elevation and current sensors close to the reflection point holds the promise of avoiding these problems and is therefore likely to be a better method for estimation of coastal reflection. However, it has been suggested (Tatavarti et al. 1988) that the reflection coefficients obtained in this way are biased towards unity by noise.

The purpose of this paper is therefore to investigate two simple techniques for estimating frequency-dependent reflection coefficients from collocated elevation and current sensors close to the reflection point, using simulated time series. The writers' simulation experiments, briefly summarized in Huntley et al. (1995), are here described in more detail and expanded to permit the establishment of confidence limits for zero reflection coefficient and also bias values for different conditions. The techniques are also applied to some field data to demonstrate their value in interpreting the results.

PRINCIPLES

"Time Domain" Approach

Guza and Bowen (1976) used the fact that for a progressive wave the orbital velocity in the direction of propagation is in phase with the elevation to propose a separation of the incoming wave elevation, η_i, and outgoing elevation, η_o, of the form:

$$\eta_i(t) = \frac{\eta(t) + (c/g)u(t)}{2} \tag{1}$$

$$\eta_o(t) = \frac{\eta(t) - (c/g)u(t)}{2} \tag{2}$$

where $\eta(t)$ = elevation time series; $u(t)$ = wave orbital velocity time series in the propagation direction (positive for incoming flow); and the factor (c/g) transforms the velocity time series into an equivalent elevation time series. The assumption here is that the waves are all traveling in the shore-normal (x-) direction, and the method therefore applies to measurements made close to the shoreline, where wave refraction has caused the directional spread of waves to narrow and become essentially shore-normal.

[1]Prof., Inst. of Marine Studies, Univ. of Plymouth, Plymouth, PL4 8AA, U.K.

[2]Res. Fellow, Dept. of Civ. and Struct. Engrg., Univ. of Plymouth, Plymouth, PL4 8AA, U.K.

[3]NPOL Naval Base, Cochin 682004, India.

Note. Discussion open until July 1, 1999. To extend the closing date one month, a written request must be filed with the ASCE Manager of Journals. The manuscript for this paper was submitted for review and possible publication on August 11, 1997. This paper is part of the ***Journal of Waterway, Port, Coastal, and Ocean Engineering***, Vol. 125, No. 1, January/February, 1999. ©ASCE, ISSN 0733-950X/99/0001-0046–0052/ $8.00 + $.50 per page. Paper No. 16428.

J. Waterway, Port, Coastal, Ocean Eng., 1999, 125(1): 46-52

Spectra of incoming and outgoing waves can then be computed from these time series, and the frequency-dependent reflection function (FDRF), $R(f)$, is taken as the square root of the ratio of the outgoing to incoming spectra:

$$R1(f) = \sqrt{\frac{\phi_{oo}(f)}{\phi_{ii}(f)}} \tag{3}$$

where $\phi_{ii}(f)$ and $\phi_{oo}(f)$ = spectra of the incoming and outgoing waves, respectively.

Although this method is simple to use, Tatavarti et al. (1988) pointed out that (1) and (2) lead to a systematic overestimation of the reflection coefficient when noise is present in one or both of the measured time series. This positive bias of the estimated reflection coefficient arises because the spectra of the sum and the difference time series for two uncorrelated noise time series will be equal, and therefore, if dominant, would produce an apparent reflection coefficient tending to one. In the next sections the magnitude of this bias will be investigated for different signal to noise ratios.

Principal Component Analysis

As an attempt to remove the bias found in the ''time domain'' method, Tatavarti et al. (1988) argued that by using principal component analysis to separate the current and elevation time series into orthogonal eigenvector combinations, the first eigenvector would tend to extract the *correlated* part of the signals of elevation and current, leaving any noise predominantly in the second and higher eigenvectors. Tatavarti et al. (1988) applied this eigenvector or principal component analysis (PCA) technique to a number of beaches in Canada, and demonstrated that the resulting FDRFs did indeed generally provide lower values than obtained by the time domain technique, and this reduction was taken to be evidence that the technique was useful.

This PCA method involves computing the eigenvectors of the cross-spectral matrices at each frequency estimate, and using the amplitudes and phases of elevation and current in the first eigenvector, which can be denoted $H(f)$, $\theta_\eta(f)$, $U(f)$, and $\theta_u(f)$, respectively, to calculate a gain function, $G(f) = H(f)/U(f)$, and a phase angle between elevation and current, $\theta_{\eta u} = (\theta_\eta - \theta_u)$. These values are then used in a form of (3) modified as follows.

Eq. (3) can be readily written in terms of the spectra of the original elevation and current time series as

$$R1^2(f) = \frac{\phi_{\eta\eta}(f) + \phi_{uu}(f) - 2\phi_{\eta u}(f)}{\phi_{\eta\eta}(f) + \phi_{uu}(f) + 2\phi_{\eta u}(f)} \tag{4}$$

where $\phi_{\eta\eta}$ and ϕ_{uu} = spectra of elevation and current, respectively; and $\phi_{\eta u}$ = cospectrum (real part of the cross-spectrum) of elevation and current. Now, in terms of the first eigenvector values, $\phi_{\eta\eta} \sim H^2(f)$, $\phi_{uu} \sim U^2(f)$, and, assuming that elevation and current components in the first eigenfunction are perfectly correlated, $\phi_{\eta u} \sim H(f)U(f) \cos \theta_{\eta u}$. Substituting these values into (4) and dividing through by $U^2(f)$ leads to the expression

$$R2^2(f) = \frac{1 + G^2(f) - 2G(f)\cos \theta_{\eta u}(f)}{1 + G^2(f) + 2G(f)\cos \theta_{\eta u}(f)} \tag{5}$$

A principal aim of this paper is to investigate the validity of this promising but essentially untested method in relation to the other, more straightforward method.

SIMULATION METHOD

A simulated elevation time series and the associated cross-shore orbital velocity time series, converted to equivalent elevation units, each with noise added and representing known degrees of wave reflection, are needed. For a single wave frequency, ω, and incoming and outgoing waves of amplitude a_i and a_o, respectively, the elevation, η, and equivalent cross-shore current [multiplied by (c/g)], u are given by

$$\eta = a_i \cos(kx + \omega t + \phi_i) + a_o \cos(kx - \omega t + \phi_o) \tag{6}$$

$$u = -a_i \cos(kx + \omega t + \phi_i) + a_o \cos(kx - \omega t + \phi_o) \tag{7}$$

where k = radian wavenumber; ϕ_i and ϕ_o = phases of the incoming and outgoing waves, respectively; and the signs of the terms are appropriate for an offshore-directed x-axis.

For the purposes of simulation one can assume, with no loss of generality, that a_i, a_o, the equivalent time delays for the incoming and outgoing waves ϕ_i/ω and ϕ_o/ω, and the wave phase velocity ω/k are all independent of frequency. This allows one to replace the monochromatic cosine terms by normally distributed random numbers, ran(n), representing white noise in frequency space. Adding uncorrelated noise to these forms of (6) and (7) leads to the following simulated time series:

$$\eta = a_i \text{ ran}(n) + a_o \text{ ran}(n - n_o) + \varepsilon_\eta \text{ ran}(m) \tag{8}$$

$$u = -a_i \text{ ran}(n) + a_o \text{ ran}(n - n_o) + \varepsilon_u \text{ ran}(p) \tag{9}$$

where the εs represent the noise amplitudes; and the time delay, n_o, is chosen to account for the effective time delay between incoming and outgoing waves. For waves near a shoreline reflector, n_o is equivalent to the nondispersive time of travel of the waves to the reflecting point and back to the sensors.

For the simulations to be discussed, a_i is set to 1 and a_o to the true reflection coefficient. For most of the simulations it has also been assumed that $\varepsilon_\eta = \varepsilon_u$, though this assumption is not essential. All of the spectra discussed in this paper were calculated from time series of 2^n points ($n = 10-14$), in blocks of 512, overlapping by 256 points, with a Hanning window applied to each block. The number of degrees of freedom, ν, has been calculated using the formula given by Nutall (1971):

$$\nu = 3.82P - 3.24 \tag{10}$$

where P = number of nonoverlapping blocks.

There is, of course, no suggestion that the white spectra associated with the time series of (8) and (9), with a reflection coefficient independent of frequency, are simulations of real spectra. The main advantage of using the random noise forms is that each frequency estimate provides an independent estimate of the calculated reflection coefficient. Thus, for example, a mean value of the bias, and the confidence levels of the estimates, can be found, for any particular choice of noise and true reflection, by averaging over the frequencies in the spectrum. From a range of such simulations, with different choices of noise and reflection coefficients, biases and confidence levels appropriate to each frequency estimate in a true spectrum can be found.

The results of applying the techniques described in the previous section to the simulated time series of (8) and (9) are discussed in the next section.

ESTIMATION OF THE INFLUENCE OF NOISE

Time Domain Method: Eqs. (1)–(4)

Fig. 1 shows an example of a simulated FDRF using the time domain method, for time series with a true reflection of 0.3 and a noise level equal to 0.4 of the amplitude of the incoming signal, and for 119 degrees of freedom. There is a clear positive bias of 0.35 over the true reflection coefficient of 0.3. The simulation tests confirm that, as predicted, this bias is independent of the number of degrees of freedom used.

J. Waterway, Port, Coastal, Ocean Eng., 1999, 125(1): 46-52

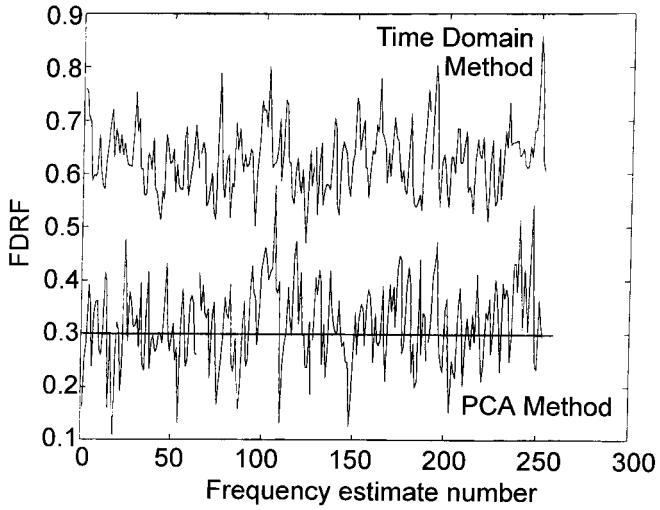

FIG. 1. Calculated Frequency-Dependent Reflection Functions (FDRFs) for True Reflection Coefficient of 0.3

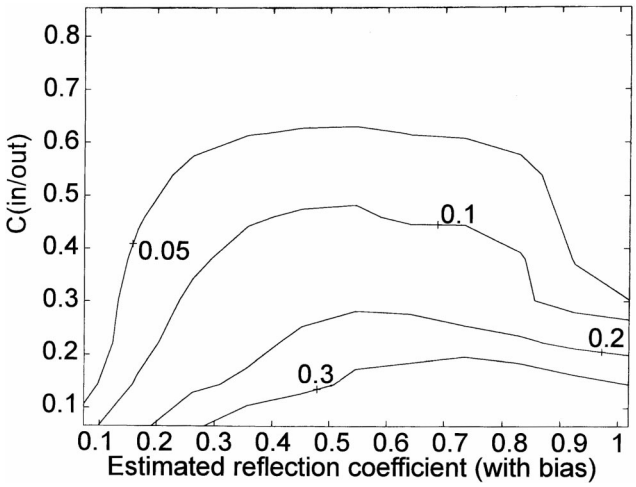

FIG. 2. Bias Values for ''Time Domain'' Method, as Function of Estimated Reflection Coefficient, Including Bias, and Corrected Coherence between Incoming and Outgoing Waves, *C*(in/out)

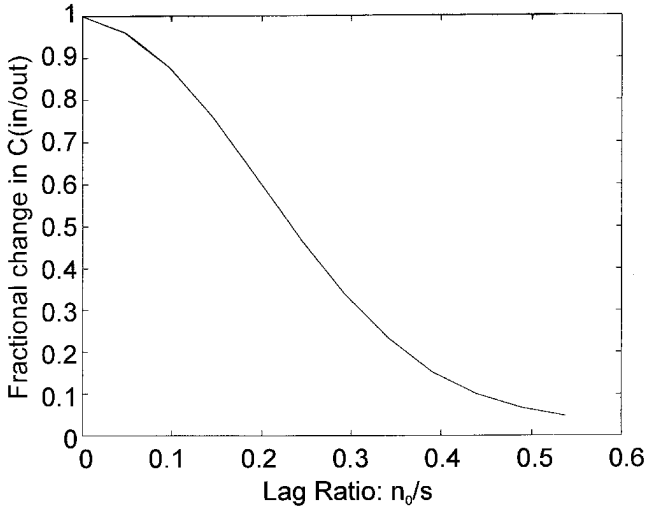

FIG. 3. Reduction in Coherence between Incoming and Outgoing Waves As Function of Ratio of Time Lag between Incoming Waves and Their Reflection, n_o, and Length of Time Series Segment Used in Spectral Analysis, *s*

In order to remove the expected bias from real data, it is necessary to be able to estimate the signal-to-noise ratio in the measurements. In the presence of reflection, the signal-to-noise ratios in the elevation and current records change systematically through the standing wave nodes and antinodes, so that coherence between elevation and current signals would be a poor estimator of noise. An alternative measure of signal-to-noise ratio is the coherence between the incoming and outgoing waves, here denoted *C*(in/out), which is not sensitive to node/antinode structure.

Fig. 2 shows the bias as a function of the *measured* reflection coefficient and the corrected incoming/outgoing wave coherence, based upon a large number of simulation tests with different true reflection coefficients and noise levels. The value of the bias clearly can become very large for small values of coherence and intermediate measured reflection coefficient. The data in this figure allow any measured value of FDRF to be corrected for bias. For operational use, the writers have developed an algorithm based on a ''look-up table'' using these data, to correct automatically the estimates of FDRF calculated by the time domain method.

However, it is important to recognize that, as it stands, Fig. 2 is only valid for measurements made very close to the reflection point, since in general *C*(in/out) depends not only on noise levels but also on the distance of the elevation and current sensors from the point of reflection. Huntley and Davidson (1998) show that decorrelation between incoming and reflected waves depends upon the ratio of the time lag between an incoming wave passing the sensors and its reflection returning to the sensors, denoted n_o in (8) and (9), and the length of time series segments used in the spectral analysis, *s*. If n_o/s is much smaller than one, the time series segments include incoming waves and their reflections, and *C*(in/out) will be high. If, on the other hand, n_o/s is large, then the time series segments will not include both incoming waves and their own reflections, and for a stochastic wave field the resulting *C*(in/out) will be low.

The writers' simulations show that, while the bias found in the time domain method is independent of the n_o/s ratio, *C*(in/out) does indeed decrease with increasing n_o/s. However, the simulations also show that the percentage decrease in *C*(in/out) is essentially only dependent on n_o/s, and is insensitive to the magnitude of the reflection coefficient and the noise level. Thus, for a known value of n_o/s, the observed value of *C*(in/out) can be ''corrected'' for this decorrelation effect, the resulting corrected value being a good measure of the noise level. Fig. 3 shows the decorrelation found through the simulations as a function of n_o/s, and can be used to make this correction, to an accuracy in the value of *C*(in/out) of better than 0.05.

Fig. 3 also illustrates the limitation on such a correction, however. For large values of n_o/s the decorrelation is large, and the corrected coherence, and associated confidence limits, become much larger than the measured values. This correction method is therefore only satisfactory for small values of n_o/s, that is, for measurements made relatively close to the reflection point. Nevertheless, as pointed out earlier, the simple methods evaluated here require shore-normal waves and therefore measurements near the shoreline, so that this additional factor is not expected to be a major limitation in practice.

Principal Component Analysis: Eq. (5)

Also shown in Fig. 1 is the result of applying the PCA method to the same simulated time series as for the time domain method. With the true reflection of 0.3, it is clear that the PCA method has removed the bias essentially to zero. The equivalent of Fig. 2 for the PCA method (not shown) shows bias values of the order of 0.02 or less across the whole parameter range, except for high reflection coefficients at low coherence (generally an unacceptable combination in reality).

J. Waterway, Port, Coastal, Ocean Eng., 1999, 125(1): 46-52

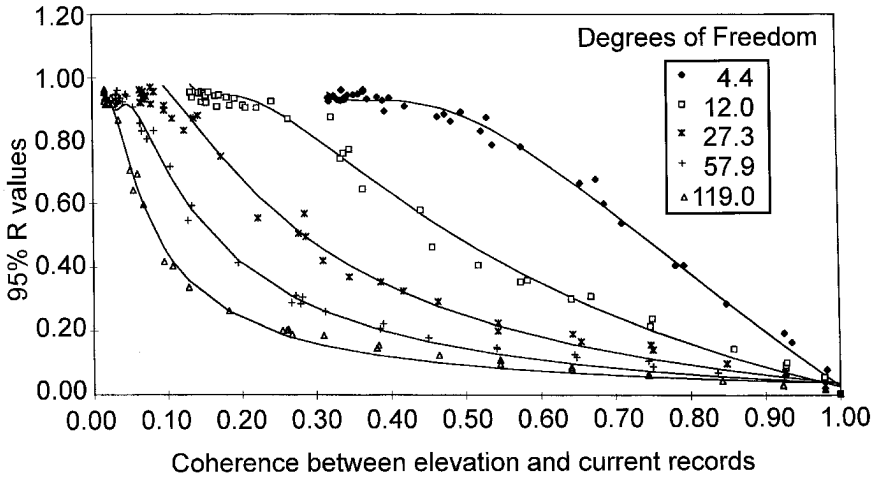

FIG. 4. 95% Confidence Levels on Zero True Reflection Coefficient As Functions of Coherence between Elevation and Current, for Different Numbers of Degrees of Freedom

TABLE 1. Coefficients for Cubic Polynomial Fits of 95% Confidence Levels versus Coherence, for Different Numbers of Degrees of Freedom

Degrees of freedom (1)	*A* (2)	*B* (3)	*C* (4)	*D* (5)	Regression coefficient (6)
4.4	—	—	—	—	—
12.0	0.0076	−0.135	0.8046	−0.649	0.993
27.3	6×10^{-4}	−0.021	0.2673	−0.208	0.994
57.9	6×10^{-5}	−0.0047	0.1195	−0.077	0.997
119.0	—	—	—	—	—

Note: The general equation takes the form: $95\%R = Acoh^{-3} + Bcoh^{-2} + Ccoh^{-1} + D$.

Perhaps unexpectedly, however, Fig. 1 shows that the PCA method has not reduced the variance of the FDRF estimates about the true value. It is also important to note that there is no evidence for any influence of standing wave nodes (expected at frequencies 60 and 190) or antinodes (expected at frequencies 0 and 130).

The clear conclusion from these analyses is that the PCA method is indeed a substantial improvement on the simple time domain method in the removal of bias due to noise. Although it involves a slightly more complex analysis, it is therefore the best method to use in estimating the FDRF from collocated elevation and current sensors.

CONFIDENCE LEVELS ON ZERO REFLECTION COEFFICIENT

The simulation technique also allows one to estimate confidence levels on the measured FDRF estimates. Here the writers estimate 95% confidence levels on zero true reflection coefficients for the PCA method for a range of degrees of freedom.

If the true reflection coefficient is zero, it is clearly inappropriate to use the coherence between incoming and outgoing waves as an indication of the signal-to-noise ratio, since there are no true outgoing waves. The writers have therefore used the coherence between the elevation and current records for this purpose. This will mean that, in application, the confidence levels will vary with the node and antinode frequencies for elevation and current, but since these variations reflect real variations in coherence, and hence signal-to-noise ratios, this approach seems justified. Distance from the reflector will have no influence on these confidence levels.

Fig. 4 shows the 95% confidence levels as functions of elevation/current coherence, for degrees of freedom ranging from 12 to 119 (4 to 32 nonoverlapping segments in the spectral analysis). The rather complex shape of the curves delineated by these data means that it has not been possible to find a universal algebraic form to model them. However cubic polynomials in the reciprocal of the coherence have been found to give close fits overall, and have been used in the assessment of the field data to be discussed later. Fits have been made separately to the data for each number of degrees of freedom, and the resulting polynomials are shown as solid curves in Fig. 4; the polynomial coefficients are given in Table 1.

CONSEQUENCES OF ELEVATION AND CURRENT SENSORS NOT BEING COLLOCATED

In practical situations it is often impossible to locate the elevation and current sensors at exactly the same horizontal location. This section considers the consequences of a time interval between a wave passing first over one sensor and then over the other. The results show that such a time interval can have very important effects on the accuracy of the resulting FDRF.

Consider the simple case of a monochromatic wave approaching normal to a shoreline reflector. For the sake of example let the current sensor be seawards of the elevation sensor, with a wave travel time of τ_x between the sensors and a further travel time of τ_s to the reflector. Assuming, as before, that the elevation (η) and current (u) records have been transformed to the same units, then for the wave components u_w and η_w:

$$\text{Incoming: } u_{wi} = a \cos \omega t; \quad \eta_{wi} = a \cos \omega(t - \tau_x) \tag{11}$$

$$\text{Outgoing: } u_{wo} = -Ra \cos \omega(t - 2(\tau_x + \tau_s)); \quad \eta_{wo} = Ra \cos \omega(t - \tau_x - 2\tau_s) \tag{12}$$

where a = amplitude of the incoming wave; R = reflection coefficient; ω = wave radian frequency; and positive velocity shorewards is assumed. The total current and elevation time series are then

$$u = u_{wi} + u_{wo} + \varepsilon_u; \quad \eta = \eta_{wi} + \eta_{wo} + \varepsilon_\eta \tag{13}$$

where the ε terms are noise contributions.

In forming estimates of the incoming and outgoing wave time series, it is appropriate to write

$$u_i = u(t) + (g/c)\eta(t - \tau); \quad u_o = u(t - \tau) - (g/c)\eta(t) \tag{14}$$

where τ = assumed time delay between the sensors. A critical consideration is the need for accuracy in the determination of

J. Waterway, Port, Coastal, Ocean Eng., 1999, 125(1): 46-52

τ_x and one therefore allows for an error, $\Delta\tau$, such that $\tau = \tau_x + \Delta\tau$. Combining (13) and (14) into (11) and (12) leads, after some manipulation, to an expression for the FDRF, denoted in this case RD, of the form

$$RD^2 = \frac{u_o^2}{u_i^2} = \frac{S^2 + R^2C^2 - 2RSC \sin \omega(\tau_x - 2\tau_s) + \varepsilon^2}{C^2 + R^2S^2 - 2RSC \sin \omega(\tau_x + 2\tau_s) + \varepsilon^2} \quad (15)$$

where

$$S = \sin \frac{\omega\Delta\tau}{2}; \quad C = \cos \omega \left(\frac{\Delta\tau}{2} + \tau_x\right); \quad \varepsilon^2 = \frac{\varepsilon_\eta^2 + \varepsilon_u^2}{a^2}$$

This general form allows one to investigate the rather unexpected influence of τ_x, $\Delta\tau$, and ε.

Consider first the case of $\Delta\tau = 0$. With $S = 0$, (15) reduces to

$$RD^2 = \frac{R^2C^2 + \varepsilon^2}{C^2 + \varepsilon^2} \quad (16)$$

and clearly in the absence of noise the correct reflection coefficient is obtained. However, with noise present, *RD* tends to one when $C = 0$, i.e., when $(2n + 1)\omega\tau_x = \pi/2$, with $n = 0, 1. \ldots$ Thus, regardless of the true reflection coefficient, *RD* will become one at frequencies

$$f = (2n + 1)/(4\tau_x) \quad (17)$$

Generally it will be important to ensure that this spurious value of reflection coefficient occurs at as high a frequency as possible, which implies that τ_x should be made as small as possible.

To illustrate this effect, Fig. 5 shows both predicted [(15)] and simulated FDRFs for two values of the noise-to-signal ratio and a true reflection coefficient of 0.4. A time delay between the sensors of one sampling interval is assumed—so that the peak [(17) for $n = 0$] occurs at half the Nyquist frequency—and the simulations use the time domain method. Clearly the peak influences a substantial frequency band, with the affected band increasing in width with increasing noise.

To give a particular example of the application of (17), if one requires the spurious peak to occur at a frequency no lower than 1 Hz, in order to ensure that the rise toward the peak does not significantly contaminate the incident wave band, then the largest separation between the sensors, in the direction of wave travel, must not exceed 0.39 m.

Unfortunately, the PCA method appears to have little effect on the influence of this peak. A PCA correction has been applied by forming the incoming and outgoing time series using the principal component values of elevation and current in (14), and then reforming equivalent elevation and current time series from the sum and difference of these. The results show the expected reduction in bias but only a small reduction in the rise of apparent reflection coefficient towards the peak.

Any error in the estimation of the time interval between the sensors creates even more drastic problems. For a true reflection coefficient of zero, (15) shows that a peak in *RD* occurs when the cosine term in the denominator goes to zero, and takes the value

$$RD^2_{\text{peak}} = 1 + \sin^2 \left(\frac{\omega\Delta\tau}{2}\right) \frac{a^2}{\varepsilon_\eta^2 + \varepsilon_u^2} \quad (18)$$

Thus the error creates a peak height greater than one. This is illustrated in Fig. 6, where an error of only one-fifth of a sampling interval (equivalent to an error in spacing of 0.08 m for the foregoing example) and a noise-to-signal ratio of only 0.125 are seen to increase the peak by nearly 30%. For nonzero true reflection coefficients, simulations show that the estimated FDRF can vary wildly and cease to resemble the true

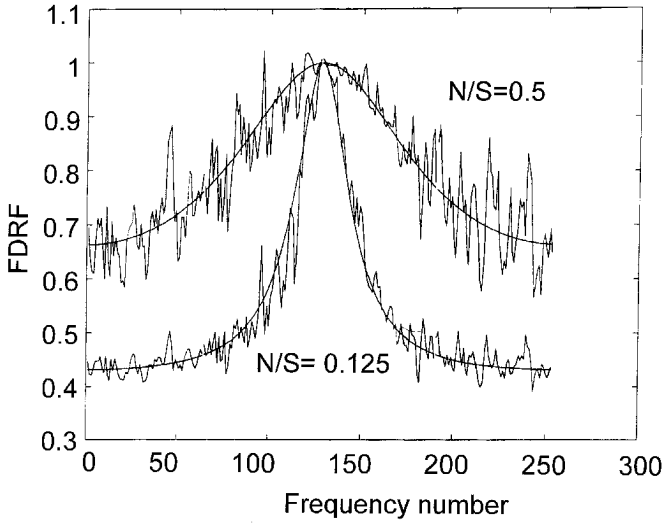

FIG. 5. Predicted (Smooth Curves) and Simulated (Jagged Curves) Values of FDRF for Two Values of Noise-to-Signal Ratio (*N/S*), True Reflection Coefficient of 0.4, and Time Delay between Elevation and Current Sensors Equal to One Digitizing Time Interval

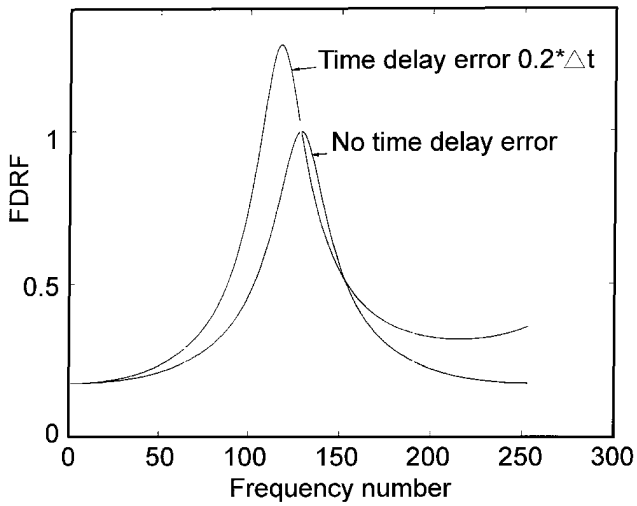

FIG. 6. Predictions of FDRF for True Reflection Coefficient of Zero and Noise Amplitude 25% of Incoming Signal Amplitude, for True Time Delay between Sensors of One Digitizing Interval, with No Error in Assumed Time Delay, and with Error of One Fifth of Digitizing Time Interval

reflection coefficient at all. In practice the true time interval between sensors can best be found by adjusting the assumed lag until the spurious peak height is minimized.

Rather similar spurious peaks can arise if output filters in the elevation and current sensors are unmatched, causing a time difference in sensor response. However, this problem, if it occurs, is much more tractable than the delays due to noncollocation since the time difference is in one direction, regardless of incoming or outgoing wave direction. It can therefore be corrected for directly in the elevation and/or current time series, generally by adjusting the phases of the Fourier transforms of the time series.

APPLICATION TO FIELD DATA

To illustrate the application of the results of this investigation to field data, measurements are used that were collected from collocated pressure and current sensors deployed on Somo sand spit, Santander, Spain, as part of an EU MAST (Marine Science and Technology) project. Currents were mea-

J. Waterway, Port, Coastal, Ocean Eng., 1999, 125(1): 46-52

sured using an electromagnetic current meter 0.1 m above the bed, and a pressure sensor mounted beneath the current meter. These sensors were approximately 50 m from the high-water line, on a beach face of slope 2.5% and high-water-line berm slope of about 4%, so that they were covered for about 2.5 h over high tide. Data were collected at 8 Hz for record lengths of 8,192, corresponding to runs of about 17 min.

Pressure data were converted to equivalent elevation, and current to equivalent elevation, using linear wave theory. Although some of the higher-frequency motion in the incident wave spectrum is likely to be forced rather than free harmonics of the primary frequency, in the shallow water conditions all wave phase velocities were very close to the shallow water limit, and hence errors in treating all wave frequencies as free waves were minimal. Although for these data the filters in the current and pressure sensors were not matched, great care was taken to measure the filter characteristics and correct for the differences by digital filtering of the time series.

Fig. 7 shows the FDRF calculated for one run using the two methods discussed. The general shape of the FDRF has low reflection at high frequencies and relatively high reflection at low frequencies, but there are substantial differences between the methods. As expected, the time domain method produces higher apparent FDRF throughout the frequency range.

Fig. 8 shows the FDRF for a second run at Somo beach, this time with the 95% confidence level on zero reflection, based upon the cubic function of the elevation/current coherence given in Table 1. The spectra of elevation and equivalent current are also shown for this run. Again the FDRF shows low reflection at high frequencies, and the confidence level suggests that it is not significantly different from zero for most of the high-frequency band. At low frequencies, the confidence level rises due to decreased coherence. The peak in the confidence level corresponds to a dip in the current spectrum and a peak in the elevation spectrum, suggesting a current node. Nevertheless, the FDRF at low frequencies is well above the 95% confidence level, so its rise toward lower frequencies is clearly real.

These results are being followed up in an investigation of the form of shoreline reflection for a variety of conditions and at a number of contrasting beach sites, in order to provide a reliable method of predicting the FDRF on natural and man-made coastlines.

As discussed in the introduction to this paper, use of collocated elevation and current sensors has important advantages over the use of spatial arrays of either sensor when coastal reflection is being estimated. The results and conclusions discussed in this paper provide the basis for accurate and statistically sound estimates of FDRFs to be made by this method.

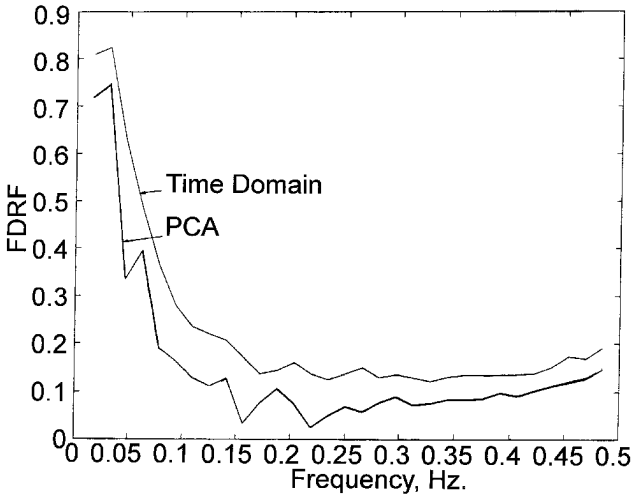

FIG. 7. FDRF for Field Data from Somo Sand Spit, Santander, Spain, Calculated by the Two Methods Reviewed in This Paper

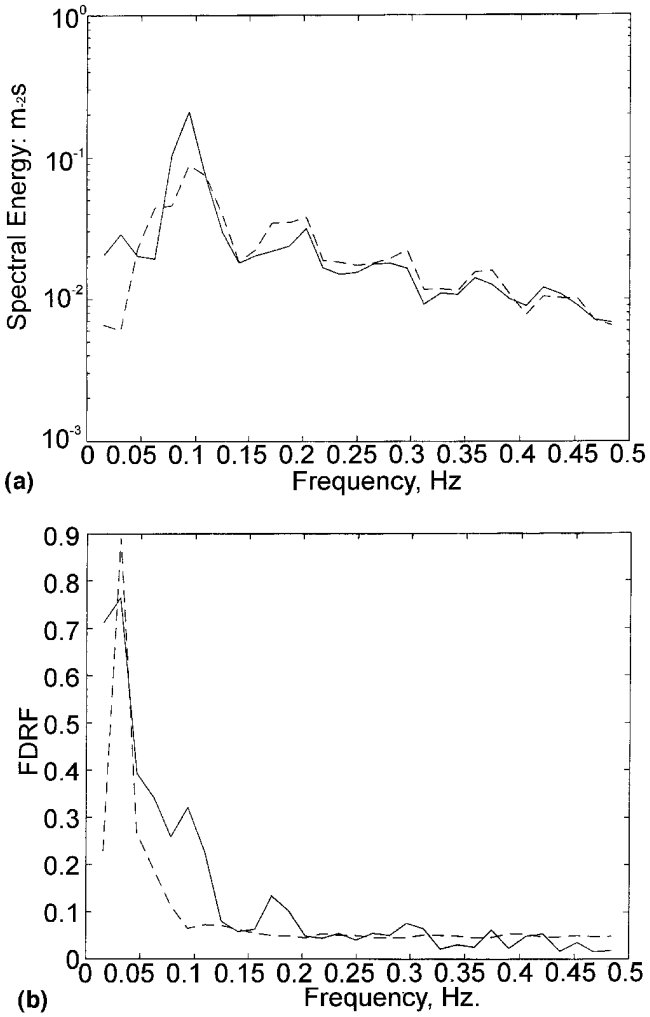

FIG. 8. Results from Second Set of Field Data: (a) Spectra of Elevation (Dashed Line) and Current (Solid Line); (b) FDRF (Solid Line) Calculated Using PCA Method, and 95% Confidence Level on Zero Reflection Coefficient (Dashed Line)

ACKNOWLEDGMENTS

The writers have benefited from discussions with Mark Davidson on the material in this paper. The field data presented here are a very small part of a large field campaign that would not have been possible without the hard work and friendship of a beach team from the University of Cantabria in Santander, Spain, led by Cesar Vidal from Miguel Losada's group. The writers acknowledge with thanks funding for this research from the European Community MAST program, under the contract ''Reflection of Waves from Natural and Man-made Coastal Structures,'' No. MAS2-CT92-0030, with support also from the contract ''Circulation and Sediment Transport around Banks,'' No. MAS2-CT92-0024.

APPENDIX I. REFERENCES

Baquerizo, A., Losada, M. A., Smith, J. K., and Kobayashi, N. (1997). ''Cross-shore variation of wave reflection from beaches.'' *J. Wtrwy., Port, Coast., and Oc. Engrg.*, ASCE, 123(5), 274–279.

Davidson, M. A., Bird, P. A. D., Bullock, G. N., and Huntley, D. A. (1996). ''A new non-dimensional number for the analysis of wave reflection from rubble mound breakwaters.'' *Coast. Engrg.*, 28, 93–120.

Elgar, S., Herbers, T. H. C., and Guza, R. T. (1994). ''Reflection of ocean surface gravity waves from a natural beach.'' *J. Phys. Oceanography*, 24(7), 1503–1511.

Frigaard, P., and Brorsen, M. (1995). ''A time-domain method for separating incident and reflected irregular waves.'' *Coast. Engrg.*, 24, 205–215.

Guza, R. T., and Bowen, A. J. (1976). ''Resonant interactions for waves

J. Waterway, Port, Coastal, Ocean Eng., 1999, 125(1): 46-52

breaking on a beach.'' *Proc., 15th Conf. on Coast. Engrg.*, ASCE, New York, 560–579.
Huntley, D. A., and Davidson, M. A. (1998). ''Estimating the directional spectrum of waves near a reflector.'' *J. Wtrwy., Port, Coast., and Oc. Engrg.*, ASCE, 124(6), 312–319.
Huntley, D. A., Simmonds, D. J., and Davidson, M. A. (1995). ''Estimation of frequency-dependent reflection coefficients using current and elevation sensors.'' *Proc., Coast. Dyn. '95*, ASCE, New York, 57–68.
Kajima, R. (1969). ''Estimation of incident wave spectra under the influence of reflection.'' *Proc., 13th Congr.*, Vol. 5.1, International Association for Hydraulic Research, Delft, The Netherlands, 285–288.
Nutall, A. H. (1971). ''Spectral estimation by means of overlapped FFT processing of windowed data.'' *Naval Underwater Sys. Ctr. Rep. No. 4169 (and supplement NUSC TR-4169S)*, New London, Conn.
Tatavarti, R. V. S. N., Huntley, D. A., and Bowen, A. J. (1988). ''Incoming and outgoing wave interactions on beaches.'' *Proc., 21st Conf. on Coast. Engrg.*, ASCE, New York, 136–150.

APPENDIX II. NOTATION

The following symbols are used in this paper:

a = wave amplitude;
a_i = incoming wave amplitude;
a_o = outgoing wave amplitude;
C = cosine term for noncollocated sensors [Eq. (16)];
C(in/out) = coherence between incoming and outgoing waves;
c = wave phase velocity;
coh = coherence between elevation and current (Table 1);
f = wave frequency (Hz);
$G(f)$ = gain function [$=H(f)/U(f)$];
g = gravitational acceleration;
$H(f)$ = amplitude of the elevation component in first PCA eigenfunction;
k = radian wave number;
m, n = integers;
n_o = time interval, in sampling intervals, between incoming and reflected waves passing sensors;
P = number of nonoverlapping blocks used in spectral analysis;
p = integer;
$R(f)$ = true frequency-dependent reflection coefficient;
$R1(f)$ = estimate of $R(f)$ using time domain method;
$R2(f)$ = estimate of $R(f)$ using PCA method;
$RD(f)$ = estimate of $R(f)$ for noncollocated sensors;
S = sine term for noncollocated sensors [Eq. (16)];
s = length of segments used in spectral analysis, in units of sampling interval;
t = time;
$U(f)$ = amplitude of current component in first PCA eigenfunction;
$u(t)$ = measured current time series;
$u_i(t)$ = incoming wave current time series;
$u_o(t)$ = outgoing (reflected) wave current time series;
u_{wi}, u_{wo} = true (noise-free) incoming and outgoing wave currents at frequency ω;
x = cross-shore axis;
$\Delta\tau$ = error in time delay between noncollocated sensors;
ε_η, ε_u = noise levels for elevation and current, respectively;
$\eta(t)$ = elevation time series;
$\eta_i(t)$, $\eta_o(t)$ = estimated incoming and outgoing elevation time series;
$\eta_{wi}(t)$, $\eta_{wo}(t)$ = time series of true (noise-free) elevation at frequency ω;
$\theta_u(f)$, $\theta_\eta(f)$ = phases of current and elevation, respectively, in first PCA eigenfunction;
$\theta_{\eta u}(f)$ = $(\theta_\eta - \theta_u)$;
ν = number of degrees of freedom;
τ_s = time delay between sensor and reflector (at wave phase velocity);
τ_x = time delay between noncollocated sensors;
ϕ_i, ϕ_o = phases of incoming and outgoing waves, respectively;
$\phi_{ii}(f)$, $\phi_{oo}(f)$ = spectra of incoming and outgoing waves, respectively;
$\phi_{\eta u}(f)$ = measured cospectrum between elevation and current;
$\phi_{\eta\eta}(f)$, $\phi_{uu}(f)$ = measured spectra of elevation and current, respectively; and
ω = wave radian frequency ($=2\pi f$).

J. Waterway, Port, Coastal, Ocean Eng., 1999, 125(1): 46-52